frontiers | Frontiers in Materials

TYPE Original Research
PUBLISHED 19 April 2023
DOI 10.3389/fmats.2023.1180345

OPEN ACCESS

EDITED BY
Chun-Xu Qu,
Dalian University of Technology, China

REVIEWED BY
Fei Cai,
Gunma University, Japan
Baokui Chen,
Nanchang University, China

*CORRESPONDENCE
Meihua Bian,
bian_mh.sy@gx.csg.cn,
gxdwxm@126.com

SPECIALTY SECTION
This article was submitted to Smart Materials, a section of the journal Frontiers in Materials

RECEIVED 06 March 2023
ACCEPTED 17 March 2023
PUBLISHED 19 April 2023

CITATION
Bian M, Peng J, Zhang X, Li J and Qin S (2023), Bearing capacities of single piles under combined *HM* loading near slopes. *Front. Mater.* 10:1180345.
doi: 10.3389/fmats.2023.1180345

Bearing capacities of single piles under combined *HM* loading near slopes

Meihua Bian*, Jianing Peng, Xingsen Zhang, Junhua Li and Songlin Qin

Guangxi Key Laboratory of Intelligent Control and Maintenance of Power Equipment, Electric Power Research Institute of Guangxi Power Grid Co., Ltd., Nanning, China

Piles are widely used to transfer the horizontal load of high-rise buildings, transmission towers, and bridges, especially for superstructures constructed near slopes. This study investigated bearing capacities of single piles under the combined horizontal force (*H*) and bending moment (*M*) for the pile in sloping ground. A 3D finite element model was proposed to simulate the non-linear pile–soil interaction and was verified by a model test. A series of numerical tests were conducted to obtain the failure envelope of bearing capacities of single piles under various combinations of *H* and *M*. The existence of slopes significantly reduced the bearing capacity of piles, especially when the horizontal and rotational displacements moved to the dip direction of the slope. An oblique ellipse was able to describe the failure envelope of bearing capacities of single piles near slopes in the *HM* plane. As the pile was installed away from the crest of the slope, both the width and height of the ellipse increased and the center of the ellipse was approaching the origin. The results of this article can provide useful references for designing horizontally loaded piles near slopes.

KEYWORDS

laterally loaded pile, slope, loading path, failure envelope, bearing capacity

1 Introduction

Single piles are designed to resist horizontal loads in geotechnical and marine engineering, offering the advantages of easy installation, low cost, good stability, and sufficient strength and stiffness (Xu et al., 2013; Xu et al., 2017a; Xu et al., 2017b; Qu et al., 2019). In particular, the piles are necessary for power transmission towers built near slopes. Due to the excitation of winds and earthquakes (Qu et al., 2018a; Qu et al., 2018b; Xu et al., 2021; Xu et al., 2023), the piles are frequently subjected to the combined horizontal force (*H*) and bending moment (*M*) (Wakai et al., 1999; Ng and Zhang, 2001; Raj et al., 2019; Yi et al., 2022). Moreover, the existence of a slope could lower the bearing capacity and thus cause instability of the piles (Jiang et al., 2022). Figure 1 shows the potential geo-hazard of the pile foundation of a transmission tower built near a slope in Baise city, Guangxi province of China. Thus, it is of great importance to study bearing capacities of single piles under combined *H* and *M* near slopes.

A pioneering study mainly focuses on single piles subjected to horizontal loading on level ground (Broms, 1964a; Broms, 1964b). Specifically, Broms (1964a, 1964b) developed an analytical formula of the ultimate soil resistance for laterally loaded flexible and rigid piles. Meyerhof (1995) developed a theoretical formula for predicting the ultimate soil resistance and bending moment of single piles under various load eccentricities and pile inclinations. In

FIGURE 1
Potential geo-hazard of the pile foundation of a transmission tower built near a slope in Baise city, Guangxi province of China (photograph from the investigation of authors).

recent years, plenty of methods have been developed to predict the lateral response of single piles near slopes. The *p*–*y* method was originally developed by Matlock (1970) and Reese et al. (1974) for analyses of laterally loaded single piles, where *p* represents the soil reaction and *y* the lateral displacement of piles. Recently, some *p*–*y* curves consider the effect of a slope on the lateral response of single piles (Georgiadis and Georgiadis, 2012; Said et al., 2020). However, the *p*–*y* method neglects the soil continuity and the soil shearing resistance (Xu et al., 2013; Xu et al., 2017a; Xu et al., 2017b). To overcome this limitation, a strain wedge model was initially developed by Norris (1986). The strain wedge (SW) model predicts the soil resistance in the passive wedge developed in front of the laterally loaded pile by introducing a stress–strain relationship for the soils in the wedge. Recently, the SW model has been extensively modified to calculate the lateral soil resistance for single piles on level ground (Xu et al., 2013; Xu et al., 2017a; Xu et al., 2017b) and in the sloping ground (Peng et al., 2019; Yang et al., 2019; Chen et al., 2021; Chen et al., 2022; Lin et al., 2022a; Hemel et al., 2022). However, the application of the SW model to obtain the failure envelope of the bearing capacities of single piles is not reported. Thus, the 3D finite element method has an advantage of considering the 3D non-linear soil–pile interaction and thus is frequently applied to estimate the lateral response of pile foundations. Accordingly, Hung and Kim (2014) and Li et al. (2014) investigated the three-dimensional failure envelope through radial displacement and sliding tests as a means to assess the safety of the pile–soil system.

The influence of a slope on the bearing capacity of piles subjected to horizontal loading has been investigated *via* either a model test or numerical test. Begum and Muthukkumaran (2009) and Perumalsamy and Ranganathan (2022) experimentally investigated the influence of the slope angle and the relative density of soils on laterally single piles. The results indicated that these two factors have a significant influence on the lateral response of single piles. In addition, recent studies experimentally investigate other influential factors, such as the embedment depth of piles, the adhesion at the pile–soil interface, the pile length, and the distance (d_{pc}) from the pile to the crest of the slope (Georgiadis et al., 2013; Deendayal et al., 2016; Vali et al., 2019). To supplement model tests, numerical analyses are conducted on laterally loaded piles in sloping ground. For example, Lin et al. (2022b) investigated the effect of various slope factors, e.g., the slope height, the slope angle, and d_{pc} on the deflection and maximum bending moment of piles. Moreover, Jiang et al. (2018) studied the influence of the loading direction on the lateral response of single piles in sloping ground *via* the 3D finite element model. Jiang et al. (2020) further numerically investigated the effect of the slope proximity and pile shape on the deflection and the bending moment of laterally loaded piles. Previous studies show that the diameter and the embedment of piles also significantly affect not only the bearing capacity but also the lateral deflection and bending moment of laterally loaded piles (Muthukkumaran and Almas, 2011; Sawant and Shukla, 2014; Rathod et al., 2019; Chandaluri and Sawant, 2020; Deendayal et al., 2020). However, little work has been carried out on the influence of the slope on the failure envelope of bearing capacities of single piles near slopes, especially under combined *HM* loading.

This study conducted 3D finite element analyses of single piles in homogeneous sandy soils near slopes under combined *HM* loading.

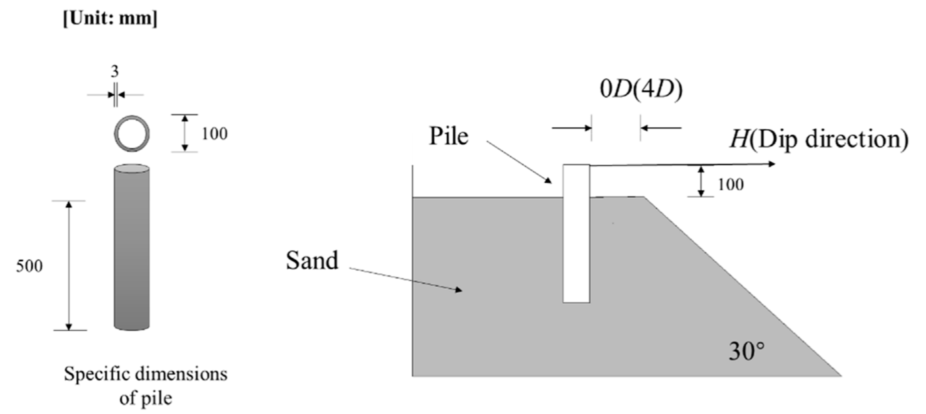

FIGURE 2
Setup of the model test on laterally loaded piles [adapted from Chae et al. (2004)].

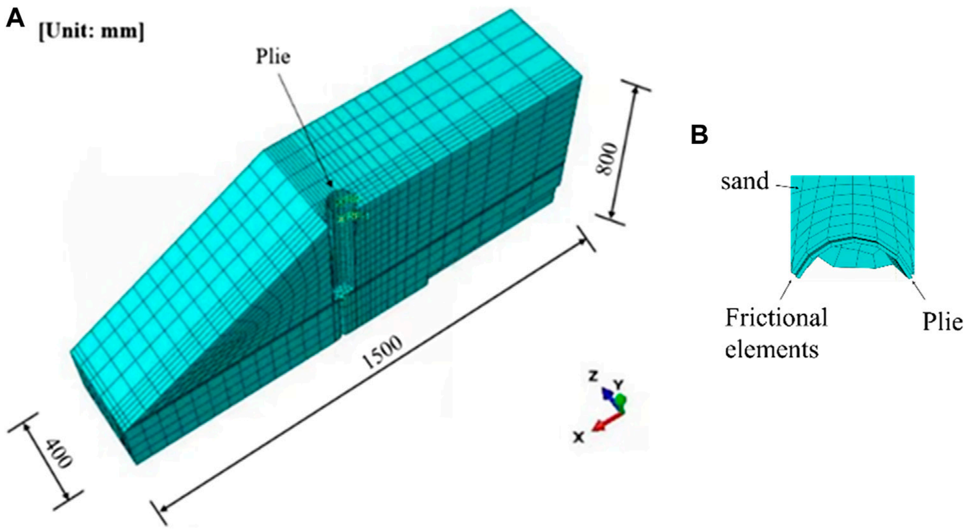

FIGURE 3
Symmetric 3D finite element model of the single pile near a sandy slope: **(A)** overall model; **(B)** the pile–soil interface modeled by frictional elements.

The 3D finite element model was calibrated against a model test reported by Chae et al. (2004). A parametric study was performed to obtain the failure envelope of bearing capacities of single piles under various combinations of H and M. The effects of the slope and d_{pc} on the failure envelope were discussed. Moreover, a formulation was proposed to describe the failure envelope of bearing capacities of single piles.

TABLE 1 Input parameters for the pile–soil system.

Model	Pile	Sand	Pile–soil interface
Unit weight γ (kN/m^3)	26.4	15.7	15.7
E (kPa)	6.86E+07	Eq. 1	Eq. 1
ν	0.345	0.3	0.3
ϕ (deg.)	—	47.5	25
ψ (deg.)	—	17.5	0

2 Numerical modeling

2.1 Description of model tests

Figure 2 shows the model test conducted on a single pile near a slope. The model test was reported by Chae et al. (2004) where the single pile was located near a sandy slope with a slope angle of 30°. The pile was a hollow steel pipe pile with an outer diameter (D) of 100 mm and a wall thickness of 3 mm. The pile

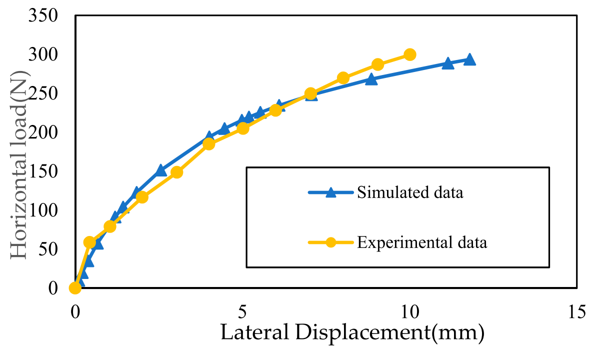

FIGURE 4
Comparisons between simulated and the measured load–displacement curves (experimental data from Chae et al., 2004).

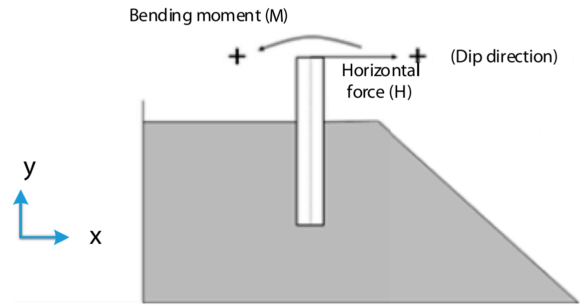

FIGURE 5
Sign definition for the bending moment and horizontal force.

was loaded horizontally with a lateral load H in the dip direction of the slope. The distance between the lateral load and the mudline was 100 mm. The embedment depth of the pile was 500 mm.

Figure 3 shows a typical symmetric 3D finite element mesh using Abaqus was used for analyzing laterally loaded single piles near the sandy slope. d_{pc} was $0D$ in this case. The single pile and the soil were modeled by C3D8R elements. The pile was assumed to behave elastically. The pile–soil interface was modeled by thin frictional elements (see Figure 3B), as suggested by Xu et al. (2023). C3D8R elements were also used for the pile–soil interface. The elastic–plastic behavior of sandy soil was described by the Mohr–Coulomb model. Table 1 lists the input parameters for the pile, the soil, and the interface. Based on triaxial compression tests of the sandy soil, the peak friction angle ϕ was 47.5° and the shear expansion angle was estimated based on the equation $\psi = \phi - 30°$ (Tatsuoka, 1993). Young's modulus E of the soil was estimated from Eq. 1 in Table 1, as suggested by Chae et al. (2004), and Poisson's ratio ν of the soil was taken as 0.3.

$$E = E_0 \left(\sigma_m / \sigma_0\right)^n, \tag{1}$$

where E_0 = 1,143 kPa, σ_0 = 1 kPa, n = 0.8311 kPa, and $\sigma_m = (\sigma_1 + \sigma_2 + \sigma_3)/3$.

The base and two lateral sides were fixed in the numerical analyses. Moreover, geostatic analysis was necessary for the slope before the lateral load was applied.

2.2 Model verification

Figure 4 shows the comparisons between simulated and the measured load–displacement curves. It should be noted that the lateral displacement was measured at the location where the lateral load was applied. The results showed that the simulated load–displacement curve agreed well with that measured from the test, demonstrating a sufficient accuracy of the proposed 3D numerical model. Accordingly, the proposed numerical model was considered a benchmark model for the following section.

3 Results and discussion

The sign convention for each direction at the top of the pile is defined in Figure 5. The positive x-axis is the dip direction of the slope. The horizontal force (H) applied in the dip direction was considered to be positive, and the bending moment (M) that forced the top of the pile to move in the dip direction was assumed to be negative.

To numerically obtain the failure envelope of bearing capacities of the single pile, both horizontal (h) and rotational (θ) displacements were applied simultaneously to the mudline, i.e., the ground surface. Moreover, the ratio of the horizontal displacement increase to the rotational displacement increase was kept constant, i.e., dh/Dθ = constant. If the pile reached the ultimate state, divergence of the finite element analyses occurred, and then, bearing capacities (H_0, M_0) were defined as the last point of the load path in the HM plane (Gottardi et al., 1999). By varying the constant dh/Dθ, the failure envelope of bearing capacities of single piles was obtained.

3.1 Failure envelope of bearing capacities of piles under combined *HM* loading near slopes

Taking the model in Figure 3 as a benchmark model ($d_{pc} = 0D$), Figure 6A shows the calculated loading paths of single piles under different constants of dh/Dd θ. The ultimate lateral load (H_0) was estimated to be 457.3 N in the dip direction when M = 0, while H_0 = −684.9 N for M = 0, where the minus sign denotes the opposite of the dip direction. This result indicated that the ultimate lateral load was reduced by 33% in the dip direction of the slope. On the other hand, the ultimate bending moment (M_0) was calculated to be 174.3 N·m in the dip direction and −245.9 N·m in the opposite dip direction when H = 0, indicating that the slope caused 29% reduction in the bearing capacity of piles.

Moreover, the maximum distance (d_{max}) between the bearing capacity (H_0, M_0) and the origin (0, 0) was achieved at positive dh/Dd θ. For example, d_{max} reached the maximum at approximately dh/Dd θ = 10. This was because the horizontal and rotational displacements caused the pile to move in opposite directions in such conditions. As dh/Dd θ decreased, the bearing capacity of piles

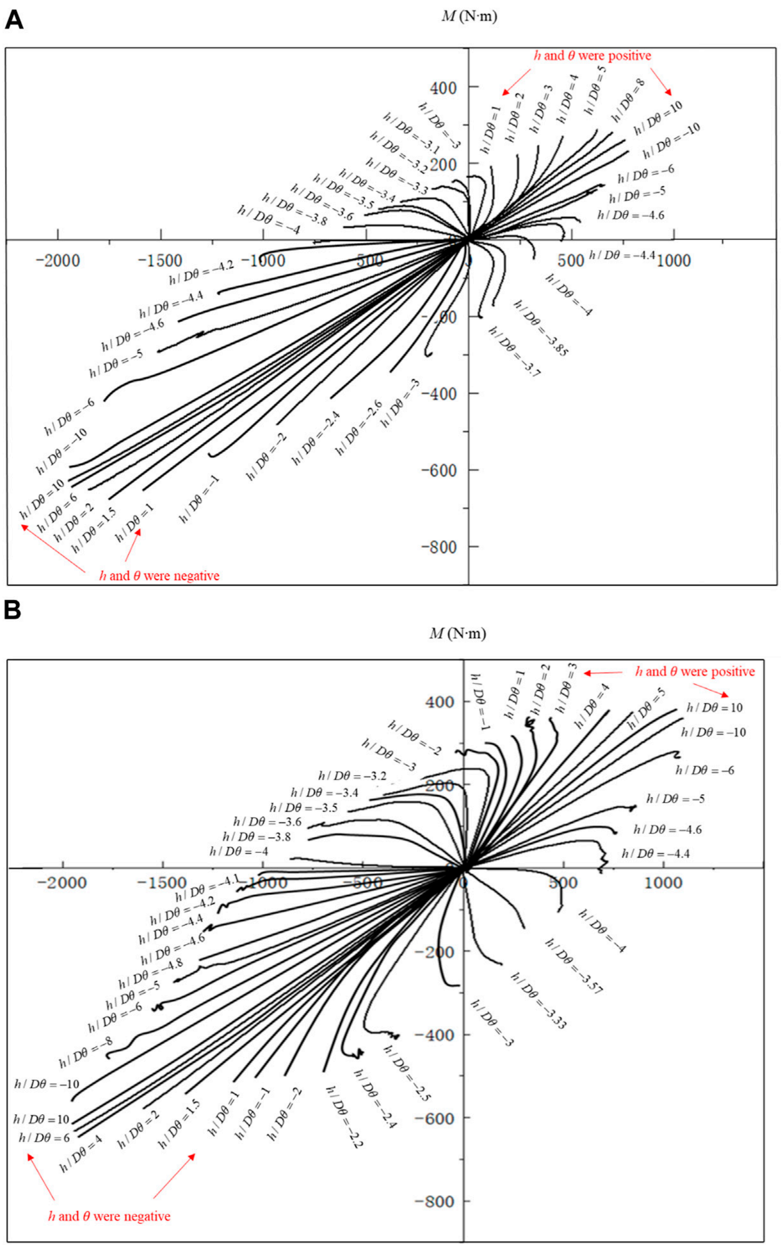

FIGURE 6
Effect of d_{pc} on the bearing capacities of loading paths of laterally loaded single piles: **(A)** d_{pc} = 0*D* and **(B)** d_{pc} = 4*D* under different constants of d*h*/D*d θ*.

generally decreased, resulting in a gradual decrease in d_{max}. d_{max} reached the minimum at negative d*h*/D*d θ*, e.g., *h*/*D θ* = −3.2. This was because the horizontal and rotational displacements caused the pile to move in the same direction. In such conditions, the failure of the pile was dominated by either the lateral load or bending moment: (1) on the loading path in the case of *h*/*D θ* = −3.6 (see Figure 6A), the horizontal load gradually increased when the bending moment reached the maximum; thus, the pile failure was mainly because of the lateral load; (2) on the loading path in the case of *h*/*D θ* = −3.85 (see Figure 6A), the bending moment gradually increased when the lateral load reached the maximum; thus, the bending moment was responsible for the failure of the pile.

From the results shown in Figure 6A, not only the slope but also the different *HM* combinations significantly affected the bearing capacity of single piles. Therefore, the most unfavorable condition should be considered in the engineering design.

3.2 Effect of the distance (d_{pc}) from the pile to the crest of the slope

To investigate the influence of d_{pc} on the bearing capacity of piles, another parallel 3D finite element model was analyzed and is shown in Figure 6. d_{pc} in this model was 4*D*, i.e., 400 mm. To eliminate the

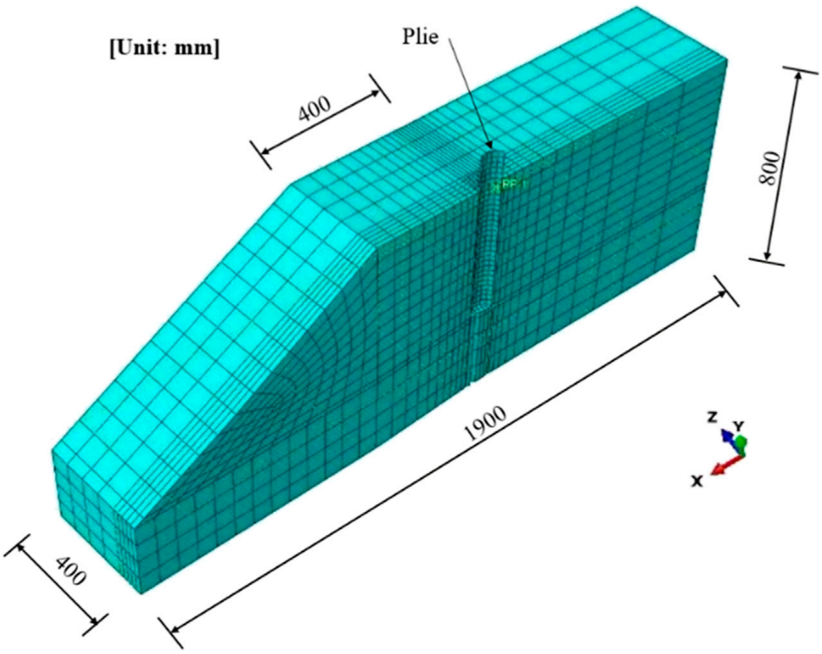

FIGURE 7
Symmetric 3D numerical model for a single pile with d_{pc} = 4D.

boundary effect, one side of the model was extended 400 mm outwards (see Figure 7). In the parallel model, input parameters were kept unchanged from the model shown in Figure 3A.

Figure 6B shows loading paths of single piles with $d_{pc} = 4D$ under different constants of dh/Dd θ. In the case of $d_{pc} = 0D$, the maximum horizontal load (H_{max}) and the maximum bending moment (M_{max}) were calculated to be −1948.8 N and −651.5 N·m, respectively (see Figure 6A). As d_{pc} increased to 4D, H_{max} and M_{max} were estimated to be −1940.8 N and −678.3 N·m, respectively (see Figure 6B). These results indicated that the effect of d_{pc} was insignificant on the maximum bearing capacity of single piles because the maximum bearing capacity depended on the soil reaction opposing the dip direction and thus was achieved when both h and θ were negative (see Figure 5). However, when both h and θ were positive, the maximum H_0 and the maximum M_0 were increased by approximately 44% and 30%, respectively, as d_{pc} increased from 0D to 4D. Moreover, both the maximum H_0 and the maximum M_0 were increased for other combinations of loading with negative dh/Dd θ due to the increase of d_{pc}. Thus, increasing d_{pc} had an insignificant effect on H_{max} but significantly increased the bearing capacity under certain loading conditions, e.g., the minimum bearing capacity.

3.3 Theoretical analysis of the failure envelope of bearing capacities of single piles in the *HM* plane

From the results shown in Figure 6, the failure envelope of bearing capacities of single piles showed an oblique ellipse in the HM plane. To verify this observation, a general elliptical equation was used to fit the data shown in Figure 6:

$$C_1x^2 + C_2xy + C_3y^2 + C_4x + C_5y + 1 = 0, \quad (2)$$

where x represents M_0 in the HM plane; y denotes the H_0 in the HM plane; and C_1, C_2, C_3, C_4, and C_5 are the constants controlling the elliptical shape. A program was developed to derive the constants from the data based on the least square method. These six constants were used to determine the coordinates of the center of the ellipse (x_0, y_0), the width and height of the ellipses R_1 and R_2, and the rotation angle of the semi-major axis ψ of the ellipse:

$$\begin{cases} x_0 = \dfrac{C_2C_5 - 2C_3C_4}{4C_1C_3 - {C_2}^2}, \\ y_0 = \dfrac{C_2C_4 - 2C_1C_5}{4C_1C_3 - {C_2}^2}, \\ R_1 = \sqrt{\dfrac{2\left(C_1{x_0}^2 + C_3{y_0}^2 + C_2x_0y_0 - 1\right)}{C_1 + C_3 + \sqrt{(C_1 - C_3)^2 + {C_2}^2}}}, \\ R_2 = \sqrt{\dfrac{2\left(C_1{x_0}^2 + C_3{y_0}^2 + C_2x_0y_0 - 1\right)}{C_1 + C_3 - \sqrt{(C_1 - C_3)^2 + {C_2}^2}}}, \\ \psi = \dfrac{1}{2}\arctan\left(\dfrac{C_2}{C_1 - C_3}\right). \end{cases} \quad (3)$$

Figures 8A, B show the failure envelope of bearing capacities of single piles near slopes for the cases with d_{pc} = 0D and d_{pc} = 4D, respectively. It should be noted that Figure 8

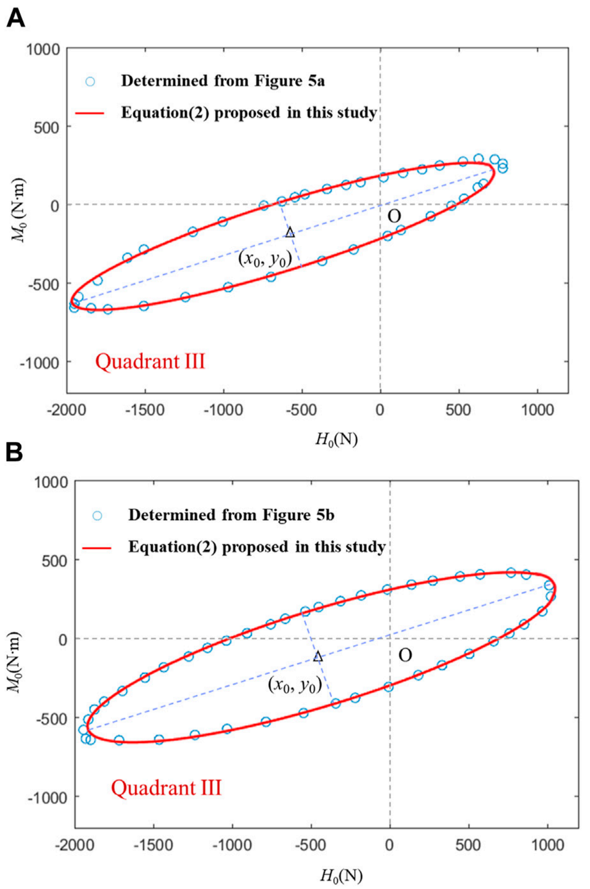

FIGURE 8
Failure envelope of bearing capacities of single piles near slopes: **(A)** d_{pc} = 0D and **(B)** d_{pc} = 4D.

was determined by collecting the last point of loading paths in Figure 6. The relationship between the horizontal load and the bending moment data can be well-described by an oblique ellipse. Table 2 gives the fitting parameters of Eq. 2. Unlike the ellipse for single piles in the level ground reported by Li et al. (2014), the center of the ellipse was not at the origin but was located in the third quadrant due to the slope effect.

Table 2 also shows that the height R_1 and the width R_2 of the failure envelope increased by 9.8% and 40.9%, respectively, as d_{pc} increased from 0*D* to 4*D*. In addition, the center of the failure envelope was much closer to the origin in the case of d_{pc} = 4*D*. Thus, the center of the ellipse was approaching the origin and the oblique ellipse became bigger as d_{pc} increased.

4 Conclusion

A 3D numerical model was proposed to accurately capture the non-linear pile–soil interaction in sloping ground and was calibrated against a model test. The conclusions are summarized as follows:

(1) The load–displacement curve simulated by the numerical model agreed well with the measured result, indicating a sufficient accuracy of the proposed 3D finite element model.
(2) An oblique ellipse can still be used to describe the failure envelope of bearing capacities of single piles near slopes in the *HM* plane. However, unlike the piles in the horizontal ground, the center of the envelope is not at the origin for piles in the sloping ground.
(3) The existence of slopes significantly reduced the bearing capacity of piles. On the other hand, the different combinations of *H* and *M* had also severely influence the bearing capacity of piles. Therefore, the most unfavorable condition should be considered in the engineering design.
(4) Increasing d_{pc} had an insignificant effect on the maximum bearing capacity of piles but could significantly increase the bearing capacity under certain loading conditions, e.g., the minimum bearing capacity.
(5) The center of the ellipse was approaching the origin, and the oblique ellipse became bigger as d_{pc} increased from 0*D* to 4*D*.

TABLE 2 Fitting results for the failure envelope of bearing capacities of single piles near slopes.

Envelope Parameter	d_{pc} = 0D	d_{pc} = 4D
Coordinates of the center (x_0, y_0)	(−614.48, −201.07)	(−429.98, −118.10)
Width R_1	1413.9	1552.5
Height R_2	215.14	303.24
Rotation angle of the semi-major axis ψ (rad)	0.3021	0.2960
Fitting parameter: C_1	−2.37E-06	−1.30E-06
Fitting parameter: C_2	1.20E-05	5.84E-06
Fitting parameter: C_3	−1.97E-05	−9.98E-06
Fitting parameter: C_4	−5.00E-04	−4.33E-04
Fitting parameter: C_5	−5.70E-04	1.51E-04

Data availability statement

The raw data supporting the conclusion of this article will be made available by the authors, without undue reservation.

Author contributions

MB: conceptualization, software, validation, and writing—original draft; JP and XZ: methodology; JL: investigation; SQ: data curation.

Funding

The authors declare that this study received funding from Electric Power Research Institute of Guangxi Power Grid Co. Ltd. of China (Grant number: GXKJXM20210299). The funder was not involved in the study design, collection, analysis, interpretation of data, the writing of this article, or the decision to submit it for publication.

Conflict of interest

Authors MB, JP, XZ, JL, and SQ were employed by the Electric Power Research Institute of Guangxi Power Grid Co., Ltd.

Publisher's note

All claims expressed in this article are solely those of the authors and do not necessarily represent those of their affiliated organizations, or those of the publisher, the editors, and the reviewers. Any product that may be evaluated in this article, or claim that may be made by its manufacturer, is not guaranteed or endorsed by the publisher.

References

Begum, N., and Muthukkumaran, K. (2009). Experimental investigation on single model pile in sloping ground under lateral load. *Int. Int. J. Geotech. Eng.* 3, 133–146. doi:10.3328/IJGE.2009.03.01.133-146

Broms, B. (1964b). Lateral resistance of piles in cohesionless soils. *J Soil Mech. Found. Div* 90, 123–156. doi:10.1061/jsfeaq.0002132

Broms, B. (1964a). Lateral resistance of piles in cohesive soils. *J Soil Mech. Found. Div* 90, 27–63. doi:10.1061/JSFEAQ.0000611

Chae, K. S., Ugai, K., and Wakai, A. (2004). Lateral resistance of short single piles and pile groups located near slopes. *Int. J. Geomech.* 4, 93–103. doi:10.1061/(asce)1532-3641(2004)4:2(93)

Chandaluri, V. K., and Sawant, V. A. (2020). Influence of sloping ground on lateral load capacity of single piles in clayey soil. *Int. J. Geotech. Eng.* 14, 353–360. doi:10.1080/19386362.2017.1419538

Chen, L., Jiang, C., Pang, L., and Liu, P. (2021). Lateral soil resistance of rigid pile in cohesionless soil on slope. *Comput. Geotech.* 135, 104163. doi:10.1016/j.compgeo.2021.104163

Chen, L., Pang, L., Jiang, C., and Zhang, C. (2022). Analysis method for bearing capacity of laterally loaded rigid piles on slopes using improved failure wedge model. *Comput. Geotech.* 145, 104700. doi:10.1016/j.compgeo.2022.104700

Deendayal, R., Muthukkumaran, K., and Sitharam, T. G. (2020). Analysis of laterally loaded group of piles located on sloping ground. *Int. J. Geomech. Eng.* 14, 580–588. doi:10.1080/19386362.2018.1448521

Deendayal, R., Muthukkumaran, K., and Sitharam, T. G. (2016). Response of laterally loaded pile in soft clay on sloping ground. *Int. J. Geotech. Eng.* 10, 10–22. doi:10.1179/1939787915Y.0000000013

Georgiadis, K., Georgiadis, M., and Anagnostopoulos, C. (2013). Lateral bearing capacity of rigid piles near clay slopes. *Soils Found.* 53, 144–154. doi:10.1016/j.sandf.2012.12.010

Georgiadis, K., and Georgiadis, M. (2012). Development of p–y curves for undrained response of piles near slopes. *Comput. Geotech.* 40, 53–61. doi:10.1016/j.compgeo.2011.09.005

Gottardi, G., Houlsby, G. T., and Butterfield, R. (1999). Plastic response of circular footings on sand under general planar loading. *Géotechnique.* 49, 453–469. doi:10.1680/geot.1999.49.4.453

Hemel, M. J., Korff, M., and Peters, D. J. (2022). Analytical model for laterally loaded pile groups in layered sloping soil. *Mar. Struc* 84, 103229. doi:10.1016/j.marstruc.2022.103229

Hung, L. C., and Kim, S. R. (2014). Evaluation of undrained bearing capacities of bucket foundations under combined loads. *Mar. Georesour. Geotec.* 32, 76–92. doi:10.1080/1064119X.2012.735346

Jiang, C., He, J. L., Liu, L., and Sun, B. W. (2018). Effect of loading direction and slope on laterally loaded pile in sloping ground. *Adv. Civ. Eng.* 1-12, 1–12. doi:10.1155/2018/7569578

Jiang, C., Liu, L., He, J. L., and Xie, H. S. (2020). Effect of the proximity of slope and pile shape on lateral capacity of piles in clay slopes. *Eur. J. Environ. Civ. Eng.* 1-15, 16–30. doi:10.1080/19648189.2020.1858452

Jiang, J. H., Huang, X. L., Shu, X. R., Ning, X., Qu, Y., and Xiong, W. L. (2022). Application of a damage constitutive model to pile–slope stability analysis. *Front. Mater* 9, 1082292. doi:10.3389/fmats.2022.1082292

Li, Z., Kotronis, P., and Escoffier, S. (2014). Numerical study of the 3D failure envelope of a single pile in sand. *Comput. Geotech.* 62, 11–26. doi:10.1016/j.compgeo.2014.06.004

Lin, M., Jiang, C., Chen, Z., Liu, P., and Pang, L. (2022a). A method for calculating lateral response of offshore rigid monopile in sand under slope effect. *Ocean. Eng.* 259, 111812. doi:10.1016/j.oceaneng.2022.111812

Lin, M., Jiang, C., Liu, P., and Pang, L. (2022b). Analysis of laterally loaded offshore pile near slope in sand considering slope height. *Ocean. Eng.* 263, 112436. doi:10.1016/j.oceaneng.2022.112436

Matlock, H. (1970). "Correlations for design of laterally loaded piles in soft clay," in Offshore Technology Conference, 577–594. doi:10.4043/1204-MS

Meyerhof, G. G. (1995). Behaviour of pile foundations under special loading conditions: 1994 R.M. Hardy keynote address. *Can. Geotech.* 32, 204–222. doi:10.1139/t95-024

Muthukkumaran, K., and Almas, B. N. (2011). Finite element analysis of laterally loaded piles on sloping ground. *Indian Geotech. J.* 41, 155–161.

Ng, C. W. W., and Zhang, L. M. (2001). Three-dimensional analysis of performance of laterally loaded sleeved piles in sloping ground. *J. Geotech. Geoenviron.* 127, 499–509. doi:10.1061/(asce)1090-0241(2001)127:6(499)

Norris, G. (1986). "Theoretically based BEF laterally loaded pile analysis," in International Conference on Numerical Methods in Offshore Piling, 361–386.

Peng, W., Zhao, M., Xiao, Y., Yang, C., and Zhao, H. (2019). Analysis of laterally loaded piles in sloping ground using a modified strain wedge model. *Comput. Geotech.* 107, 163–175. doi:10.1016/j.compgeo.2018.12.007

Perumalsamy, K., and Ranganathan, S. (2022). Single pile in cohesionless soil in sloping ground under lateral loading. *Int. J. Geotech. Eng.* 13, 8. doi:10.1186/s40703-022-00173-8

Qu, C. X., Yi, T. H., Li, H. N., and Chen, B. (2018a). Closely spaced modes identification through modified frequency domain decomposition. *Measurement* 128, 388–392. doi:10.1016/j.measurement.2018.07.006

Qu, C. X., Yi, T. H., and Li, H. N. (2019). Mode identification by eigensystem realization algorithm through virtual frequency response function. *Struct. Control Hlth.* 26, e2429. doi:10.1002/stc.2429

Qu, C. X., Yi, T. H., Zhou, Y. Z., Li, H. N., and Zhang, Y. F. (2018b). Frequency identification of practical bridges through higher order spectrum. *J. Aerosp. Eng.* 31, 04018018. doi:10.1061/(ASCE)AS.1943-5525.0000840

Raj, D., Singh, Y., and Kaynia, A. M. (2019). V–H–M seismic capacity envelopes of strip foundations on slopes for capacity design of structure-foundation system. *B. Earthq. Eng.* 17, 2963–2987. doi:10.1007/s10518-019-00577-5

Rathod, D., Muthukkumaran, K., and Thallak, S. G. (2019). Experimental investigation on behavior of a laterally loaded single pile located on sloping ground. *Int. J. Geomech.* 19, 04019021. doi:10.1061/(asce)gm.1943-5622.0001381

Reese, L. C., Cox, W. R., and Koop, F. D. (1974). "Analysis of laterally loaded piles in sand," in Offshore Technology Conference, 473–483. doi:10.4043/2080-MS

Said, S. E., Fayed, A. L., and El M, Y. (2020). P–y curves of laterally loaded piles near Earth slopes. *Int. J. Eng. Adv. Technol.* 9, 805–814. doi:10.35940/ijeat.D7763.049420

Sawant, V. A., and Shukla, S. K. (2014). Effect of edge distance from the slope crest on the response of a laterally loaded pile in sloping ground. *Geotech. Geol. Eng.* 32, 197–204. doi:10.1007/s10706-013-9694-7

Tatsuoka, F. (1993). "Relationships between stress and strain increments," in Intr. to Strength of Soils and Failure of Ground, 57–81.

Vali, R., Shams, G., Porhoseini, R., Boroujeni, M. S., and Beygi, M. (2019). Lateral behavior of pile located on top of a slope. *Aust. Geomech. J.* 54, 103–114.

Wakai, A., Gose, S., and Ugai, K. (1999). 3-D elasto-plastic finite element analyses of pile foundations subjected to lateral loading. *Soils Found.* 39, 97–111. doi:10.3208/sandf.39.97

Xu, L. Y., Cai, F., Wang, G. X., Chen, G. X., and Li, Y. Y. (2017b). Nonlinear analysis of single reinforced concrete piles subjected to lateral loading. *KSCE J. Civ. Eng.* 21, 2622–2633. doi:10.1007/s12205-017-1010-2

Xu, L. Y., Cai, F., Wang, G. X., and Chen, G. X. (2017a). Nonlinear analysis of single laterally loaded piles in clays using modified strain wedge model. *Int. J. Civ. Eng.* 15, 895–906.

Xu, L. Y., Cai, F., Wang, G. X., and Ugai, K. (2013). Nonlinear analysis of laterally loaded single piles in sand using modified strain wedge model. *Comput. Geotech.* 51, 60–71. doi:10.1016/j.compgeo.2013.01.003

Xu, L. Y., Chen, W. Y., Cai, F., Song, Z., Pan, J. M., and Chen, G. X. (2023). Response of soil–pile–superstructure–quay wall system to lateral displacement under horizontal and vertical earthquake excitations. *B. Earthq. Eng.* 21, 1173–1202. doi:10.21203/rs.3.rs-1544907/v1

Xu, L. Y., Song, C. X., Chen, W. Y., Cai, F., Li, Y. Y., and Chen, G. X. (2021). Liquefaction-induced settlement of the pile group under vertical and horizontal ground motions. *Soil Dyn. Earthq. Eng.* 144, 106709. doi:10.1016/j.soildyn.2021.106709

Yang, M., Deng, B., and Wang, Y. (2019). A simplified calculation method for the near-slope laterally loaded pile based on a passive wedge model. *Adv. Civ. Eng.* 2019, 1–10. doi:10.1155/2019/8363252

Yi, S., Liu, J., and Gu, M. (2022). Field investigation of steel pipe pile under lateral loading in extensively soft soil. *Front. Mater* 480. doi:10.3389/fmats.2022.971485